

Polymer Chemistry

Accepted Manuscript



This is an *Accepted Manuscript*, which has been through the Royal Society of Chemistry peer review process and has been accepted for publication.

Accepted Manuscripts are published online shortly after acceptance, before technical editing, formatting and proof reading. Using this free service, authors can make their results available to the community, in citable form, before we publish the edited article. We will replace this *Accepted Manuscript* with the edited and formatted *Advance Article* as soon as it is available.

You can find more information about *Accepted Manuscripts* in the [Information for Authors](#).

Please note that technical editing may introduce minor changes to the text and/or graphics, which may alter content. The journal's standard [Terms & Conditions](#) and the [Ethical guidelines](#) still apply. In no event shall the Royal Society of Chemistry be held responsible for any errors or omissions in this *Accepted Manuscript* or any consequences arising from the use of any information it contains.



Journal Name

ARTICLE

Effects of *trans*- or *cis*-cyclohexane unit on the thermal and rheological properties of semi-aromatic polyamides

Gang Zhang^{a*}, Guang-Ming Yan^a, Hao-Hao Ren^a, Yan Li^a, Xiao-Jun Wang^a, Jie Yang^{a,b*}Received 00th January 20xx,
Accepted 00th January 20xx

DOI: 10.1039/x0xx00000x

www.rsc.org/

Semi-aromatic monomers containing cyclohexane unit, prepared by the facile interfacial reaction method from the 1,4-cyclohexanediamine (*trans*- or *cis*-) and 4-fluorobenzoyl chloride (4-FBC) at room temperature, was conducted to react with 1,1-bis(4-hydroxyphenyl)-1-phenylethane (BHPPE) to afford two kinds of semi-aromatic polyamide (BH-*trans*-BFCO or BH-*cis*-BFCO) in this work. Thermal properties investigation confirmed that a high glass transition temperatures (T_g) of 224–265 °C and a good thermal stability with initial degradation temperatures (T_d) of 445 to 450 °C for the synthesized semi-aromatic polyamides, which determined by differential scanning calorimetry (DSC) and thermogravimetric analysis (TGA) characterization. It was found that the properties (thermal and mechanical properties) of BH-*trans*-BFCO containing *trans*-conformation were much better than BH-*cis*-BFCO containing *cis*-conformation. Comparing the thermal stability of the resultant semi-aromatic polyamides with commercial product PA6T-Dupont, the prepared polyamides treated at 220 °C for 7 h displayed a slighter reduce tensile strength as well as a smaller change in color. According to the rheological test, they were found to have better melt flowability (complex viscosities ranged from 210 to 3070 Pas at 310 °C to 360 °C). Additionally, their thermal degradation kinetics and thermal pyrolysis mechanism of these semi-aromatic polyamides were investigated by thermogravimetric analysis and Pyrolysis/Gas Chromatography/Mass (Py-GC/MS) analysis further indicating their higher thermal stability and processability.

Introduction

Nylon exhibits outstanding properties such as good mechanical performance and melting processability due to its good chain regularity and large content strong hydrogen bonds [1, 2]. However, the moderate thermal property limits its widely application especially when it is used in the surface mount technology (SMT) and so on. In order to improve the thermal properties of aliphatic polyamides, incorporation of aromatic units into the polymer main chain acts as an efficient approach [3-7]. Aromatic polyamides (aramids), such as Aramid-1414 and Aramid-1313, are well-known for their excellent thermal, mechanical and corrosion resistance properties as one of the irreplaceable special engineering plastics [8, 9], but with the drawback of poor processability. Therefore, semi-aromatic polyamides combining the high long-term use temperature and heat resistance of wholly aromatic polyamides with the good melting processability of nylon are preferable. However, only a few semi-aromatic polyamides, such as poly(nonamethylene terephthalamide) (PA9T) [10-14],

poly(decamethylene terephthalamide) (PA10T) [15,16] and copolymers of PA6T/66, PA6T/6 and so on [17], are commercial and processable. Usually, semi-aromatic polyamides e.g. PA4T, homopolymer of PA6T, and so on (as shown in Table 1) which contain short chain (less than 7 methylenes) diamine are found to have poor solubility and possess higher melt temperature than thermal degradation temperature. They are thought to be impossible for thermal processing. Therefore, in the past decade, much attention has focused on chemical modification of semi-aromatic polyamide to improve its processability such as incorporation of cyclodextrin unit [18], sulfide groups [19], ester unit [20, 21] and long carbon chain [22-27] [PA-10T, PA-12T and PA-18T (T_m = 245 °C) and so on] into the polymer backbone to decrease its melt temperature and improve its melt processability; or introduction of noncoplanar biphenylene moieties [28], hyperbranched units [29,30], bulky pendant groups [31-33], triazole units [34], sulphone units [35] and azo groups [36,37] into the polymer main chain to weaken its molecular regularity for improving its solution processability.

Table 1 The melt temperature (T_m) and thermal degradation temperature (T_d) of traditional semi-aromatic polyamides

Polymer	T_m (°C)	T_d (°C)	Polymer	T_g (°C)	T_m (°C)	T_d (°C)
PA4T	430	350	PA18T	-	245	-
PA6T	370	350	Semi-aromatic	270	-	500

^aInstitute of Materials Science & Technology, Analytical & Testing Center, Sichuan University, Chengdu 610064, P. R. China. E-mail: gangzhang@scu.edu.cn

^bState Key Laboratory of Polymer Materials Engineering (Sichuan University), Chengdu, 610065, P. R. China. E-mail: ppsf@scu.edu.cn

^cElectronic Supplementary Information (ESI) available: [details of any supplementary information available should be included here]. See DOI: 10.1039/x0xx00000x

(homopolymer)			PA (with bulky pendant groups)		
PA9T	305	464	PA (with biphenylene unit)	300	510
PA10T	315	472	PA (with naphthalene ring)	-	300 495
PA12T	295	429	PA (with ester unit)	110-140	219-260

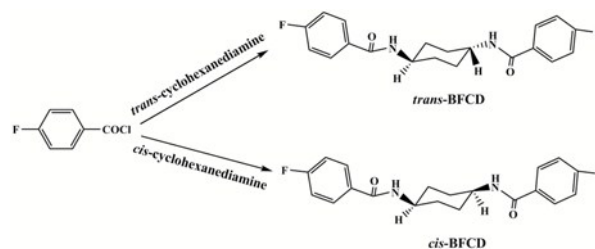
Additionally, the durability of commercial semi-aromatic such as copolymer of PA6T/66 at high temperature is found to be not well. The color of the products becomes deep, and its tensile strength decreases gradually with the treatment time under high temperature. Therefore, the aim of this work would be to synthesize the well-designed semi-aromatic polyamides with a pronounced processability, mechanics and thermal properties. In this case, we introduced the monomer containing stable cyclohexane unit (cis- or trans- conformation) into the polymer chain to investigate the polymers' thermal and rheological properties. On the other hand, the incorporation of bulky side group are expected to lower the inter-chain interaction and reduce the polymers' viscosity, so the bisphenol BHPPE containing bulky side group was conducted to react with BFCd through the nucleophilic substitution reaction in this work. Finally, the effects of different conformation on these semi-aromatic polyamides' thermal, rheological properties, degradation kinetics and mechanism were investigated in detail.

Results and Discussion

Synthesis and chemical structure of monomers (*trans*-BFCd and *cis*-BFCd)

The semi-aromatic monomers containing cyclohexane unit was synthesized with a facile interfacial reaction using dichloromethane and water as solvents. In order to avoid the generation of mono-substitution byproduct of N-(4-fluorobenzoyl) *trans*- or *cis*-cyclohexanediamine, during the reaction procedure, 4-FBC was always kept excessive by adding 1,4-cyclohexanediamine into the solution of 4-FBC. That is beneficial for getting high yield and purity of product. **Figure 1** is the FT-IR spectra of monomers, it can be found that the amide absorptions near 3300, 1635 cm^{-1} , methylene absorptions near 2930, 2850 cm^{-1} , benzene ring (C=C) absorptions near 1600 and 1490 cm^{-1} , para-substituted benzene rings absorptions near 850 cm^{-1} . The characteristic absorption of C-N in *cis*-BFCd (1233 cm^{-1}) is found to be much stronger than that of *trans*-BFCd (1228 cm^{-1}). The main reason is that *trans*-BFCd has much higher symmetry, the bond of C-N

is affected by more carbonyl unit, so the bond of C-N is weakened. The FT-IR result suggests the amidation reaction of 4-FBC and 1,4-cyclohexanediamine is occurred. **Figure 2** is the $^1\text{H-NMR}$ spectra of *trans*-BFCd and *cis*-BFCd. The proton signals of cyclohexane units are ranged from 1.42 to 3.88 ppm. The signals in the range of 7.26-7.95 ppm are attributed to proton of benzene ring. The proton signal of -CONH- is a double peak at 8.084-8.100 ppm (*cis*-BFCd) or at 8.287-8.307 ppm (*trans*-BFCd). The chemical shift of *trans*-BFCd is larger when compared to *cis*-BFCd. It is ascribed to the high content of hydrogen bond in *trans*-BFCd due to its higher symmetry than that of *cis*-BFCd (as shown in **Figure 3**), then the proton signal of N-H shifts to low-field. The chemical structure characterizations indicating the monomers are synthesized as shown in **Scheme 1**.



Scheme 1 Synthesis route of *trans*-BFCd and *cis*-BFCd.

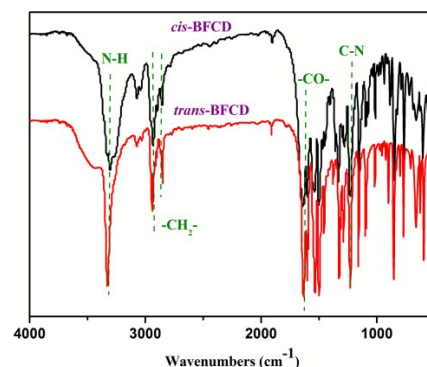


Figure 1 The FT-IR spectra of *trans*-BFCd and *cis*-BFCd.

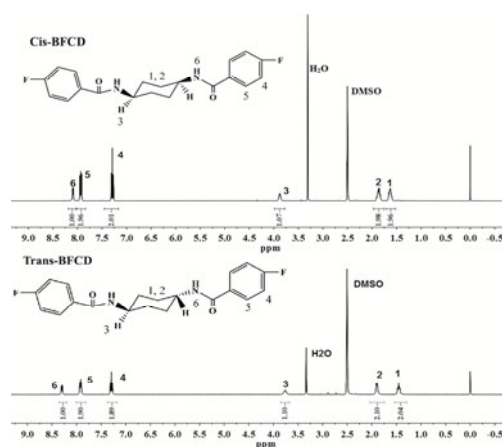
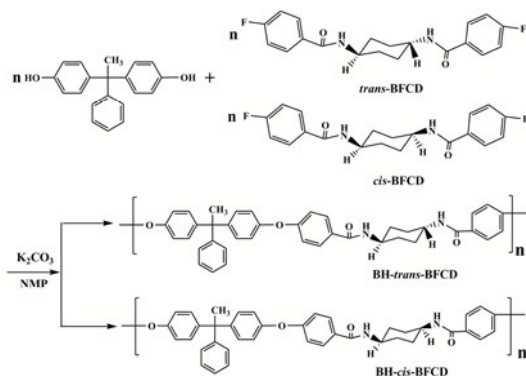


Figure 2 The $^1\text{H-NMR}$ spectra of *trans*-BFCd and *cis*-BFCd.

Synthesis and chemical structure of polymers (BH-*trans*-BFCD and BH-*cis*-BFCD)

Two kinds of novel semi-aromatic polyamides were synthesized through the reaction of bisphenol (BHPPE) and BFCD. At the prepolymerization stage, low reaction temperature was applied to carry out the byproduct water while then high temperature was maintained to yield high molecular weight polyamides in the step of polycondensation. The molecular weights of the resultant semi-aromatic polyamides were characterized by intrinsic viscosities and GPC, which are listed in **Table 2**. It is found that the molecular weight of BH-*trans*-BFCD is larger than that of BH-*cis*-BFCD. The reactivity of the polymerization reaction rate was evaluated by the model reaction of *trans*-BFCD or *cis*-BFCD with phenol (see supplementary information). The monomer of *trans*-BFCD was found to have almost the same reaction rates with *cis*-BFCD. The difference of viscosity in BH-*trans*-BFCD and BH-*cis*-BFCD may be based on their difference of hydrodynamic radius. FT-IR spectra of BH-*trans*-BFCD and BH-*cis*-BFCD are showed in **Figure 4**. The characteristic absorptions of -CONH-, -CH₂- and benzene ring were similar with the monomers. The absorption of C-F near 1330 cm⁻¹ was almost disappeared while two new characteristic absorptions near 1172 cm⁻¹ and 2960 cm⁻¹ which attributed to the absorption of ether bond and methyl unit could be observed. It suggests the nucleophilic substitution reaction of C-F and -OH is occurred. **Figure 5** is the ¹H-NMR spectrum of BH-*trans*-BFCD. The proton signals of aliphatic chain were in the range of 1.4 to 3.8 ppm. The single peak at 2.1 ppm was attributed to the proton of -CH₃. The aromatic ring proton signals appeared in the range of 6.9-7.9 ppm. They were too closed to be separated well. But the ratio of integral proton signals was about 4:4:3:2:4:4:2:1:2:4:2, which was identical with the calculated result. BH-*cis*-BFCD was also confirmed by ¹H-NMR spectrum (as shown in **Figure 6**). Comparing with the ¹H-NMR spectrum of BH-*trans*-BFCD, it was found that the proton signal of N-H showed a similar chemical shift trend as the monomers still because of the stronger role of hydrogen bond of BH-*trans*-BFCD than BH-*cis*-BFCD. The chemical structure characterizations indicating the polymers are synthesized as shown in **Scheme 2**.



Scheme 2 Synthesis route of BH-*trans*-BFCD and BH-*cis*-BFCD.

Table 2 Intrinsic viscosity (η_{int}) and molecular weights of BH-*trans*-BFCD and BH-*cis*-BFCD.

Polyamides	η_{int} (dL/g)	M_n (g/mol)	M_w (g/mol)	PDI (Mw/Mn)
BH- <i>trans</i> -BFCD	1.17	7.40×10^4	1.61×10^5	2.18
BH- <i>cis</i> -BFCD	0.93	6.12×10^4	1.46×10^5	2.39

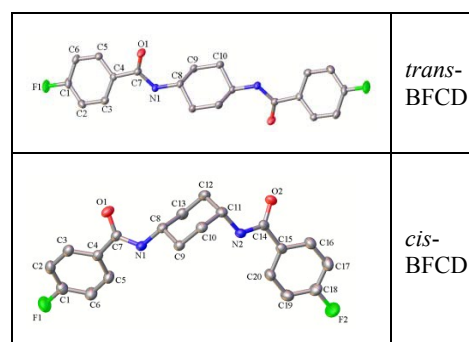


Figure 3 The molecular structure of *trans*-BFCD and *cis*-BFCD tested with Four-circle single-crystal diffraction.

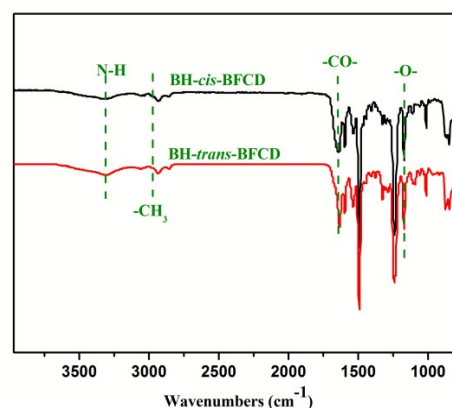


Figure 4 The FT-IR spectra of BH-*trans*-BFCD and BH-*cis*-BFCD.

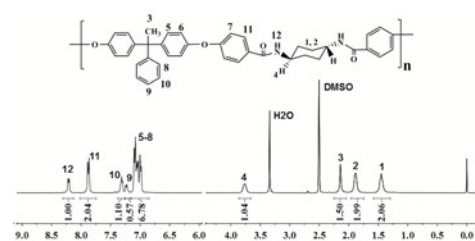


Figure 5 The ¹H-NMR spectrum of BH-*trans*-BFCD.



Figure 6 The ^1H -NMR spectrum of BH-*cis*-BFCD.

Thermal analysis of BH-*trans*-BFCD and BH-*cis*-BFCD

The thermal properties of the resultant semi-aromatic polyamides were first tested with DSC. As shown in **Figure 7**, the obvious glass transition temperature (T_g) of BH-*trans*-BFCD and BH-*cis*-BFCD around 224 and 265 °C, respectively, could be observed. The T_g of BH-*trans*-BFCD is about 40 °C higher than BH-*cis*-BFCD. The main reason is the low inter-chain interaction caused by loose packing of polymer chains and less hydrogen bond of BH-*cis*-BFCD. No melting peak was found for both polymers from the DSC curves indicating they both are amorphous. **Figure 8** is the TGA curves of BH-*trans*-BFCD and BH-*cis*-BFCD tested at different heating rates (5, 10, 20 and 40 °C/min) under nitrogen atmosphere. The starting thermal degradation temperature ($T_{d5\%}$) of BH-*trans*-BFCD and BH-*cis*-BFCD was 450 and 445 °C, respectively. The char yield of BH-*trans*-BFCD and BH-*cis*-BFCD at 800 °C in nitrogen was about 11.1 and 10.7 wt%, respectively. In order to investigate the difference of the thermal decomposition behaviour of these semi-aromatic polyamides, differential method (Kissinger method) was applied to calculate their thermal degradation kinetics. The Kissinger method can be used to calculate the activation energy (E), degradation order (n) and pre-exponential factor $\ln A$ [38], and does not need to know the degradation mechanism beforehand, with the following equation (2):

$$\ln\left(\frac{\beta}{T_{\max}^2}\right) = \left\{ \ln\frac{AR}{E} + \ln\left[n(1-\alpha_{\max})^{n-1}\right] \right\} - \frac{E}{RT_{\max}} \quad (2)$$

where β is the heating rate, T_{\max} is the maximum thermal degradation temperature, n is the reaction order, α_{\max} is the maximum conversion, A is the pre-exponential factor. The activation energy E can be calculated according to the slope from the plot of $\ln(\beta/T_{\max}^2)$ versus $1000/T_{\max}$. The values of initial decomposition temperature ($T_{d5\%}$) and the maximum thermal degradation temperature (T_{\max}) are shown in **Table 3**. **Figure 9** shows the curves of Kissinger method applied to experimental data at different heating rates. The values (as shown in **Table 4**) obtained from **Figure 9** for the activation energy (E) of BH-*trans*-BFCD and BH-*cis*-BFCD were 240.9 and 235.2 kJ/mol, respectively. BH-*trans*-BFCD displayed the highest thermal degradation activation energy among these semi-aromatic polyamides, suggesting it exhibits the best thermal stability. Comparing with BH-*cis*-BFCD, the molecular chain of BH-*trans*-BFCD consists of much more close packing

and hydrogen bond than that of BH-*cis*-BFCD, so BH-*trans*-BFCD shows the most stable thermal stability.

Table 3 The initial and maximum thermal degradation temperatures of BH-*trans*-BFCD and BH-*cis*-BFCD.

Heating rates	BH- <i>trans</i> -BFCD		BH- <i>cis</i> -BFCD	
	$T_{d5\%}$ (°C)	T_{\max} (°C)	$T_{d5\%}$ (°C)	T_{\max} (°C)
5 °C/min	438	480	438	473
10 °C/min	450	494	445	489
20 °C/min	464	509	459	505
40 °C/min	482	520	477	512

Table 4 The slope, intercept of fitting line and calculated values of E of BH-*trans*-BFCD and BH-*cis*-BFCD.

Polymers	Fitting line slope	Fitting line intercept	Activation energy E (KJ/mol)
BH- <i>trans</i> -BFCD	-28.979	26.816	240.9
BH- <i>cis</i> -BFCD	-28.284	26.210	235.2

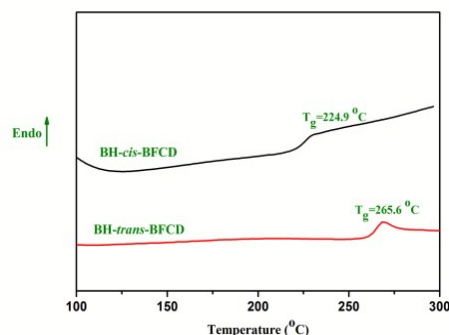


Figure 7 DSC curves of BH-*trans*-BFCD and BH-*cis*-BFCD.

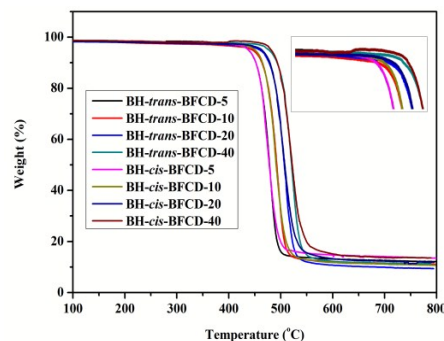


Figure 8 TGA curves of BH-*trans*-BFCD and BH-*cis*-BFCD at different heating rates.

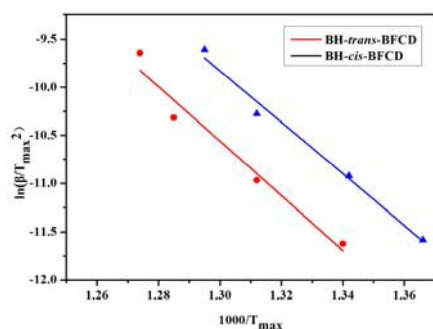


Figure 9 Kissinger method applied to experimental data at different heating rates of BH-*trans*-BFCD and BH-*cis*-BFCD.

Thermal degradation mechanism

Py-GC/MS was used to characterize the thermal degradation mechanism of BH-*trans*-BFCD, BH-*cis*-BFCD and PA6T-Dupont under nitrogen atmosphere at 550 °C and 650 °C, respectively. As shown in **Figure 10**, four kinds of degradation compounds of BH-*trans*-BFCD and BH-*cis*-BFCD such as: benzene, toluene, ethylbenzene and phenol were found at 550 °C. It was attributed to the polymer side chain decomposition and the further degradation of diphenol units. That was quite different from the decomposition routes of PA6T-Dupont. The degradation compounds of PA6T-Dupont at 550 °C were consisted of cyclopentanone, benzonitrile, methylbenzonitrile, hexanedinitrile and 1, 4-benzendicarbonitrile. The polymer main chain of PA6T-Dupont began to decompose from the amide unit while BH-*trans*-BFCD and BH-*cis*-BFCD began to degrade from the side chain of BHPPE unit. So BH-*trans*-BFCD (or BH-*cis*-BFCD) showed higher thermal stability than PA6T-Dupont. It agreed with the result of the thermal degradation kinetics analysis. The degradation compounds of BH-*trans*-BFCD, BH-*cis*-BFCD and PA6T-Dupont were up to nine kinds of products when the pyrolysis temperature risen up to 650 °C. Comparing with the first pyrolysis step, BH-*trans*-BFCD decomposed much more pieces with the increase of pyrolysis temperature such as: benzonitrile, diphenyl ether, Diphenylmethane, 1-metyl-4-phenoxy-benzene and 4-phenoxybenzonitrile. It indicates that the amide groups begin to degrade with the appearance of compounds which containing nitrile unit. In other words, it suggests that the polymer main chain of BH-*trans*-BFCD begin to decompose when the pyrolysis temperature is 650 °C. As summarized at **Table 5**, it was found that PA6T-Dupont continued to decompose into much smaller pieces (alkyl radicals) and isomerized into 4-methylbenzonitrile, ethylbenzonitrile and 4-ethenylbenzonitrile with increase of the pyrolysis temperature up to 650 °C.

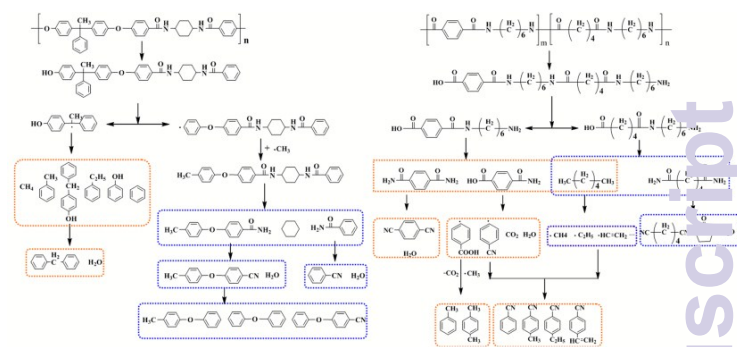


Figure 10 Thermal degradation routes of BH-*trans*-BFCD, BH-*cis*-BFCD and PA6T-Dupont.

Table 5 Thermal degradation compounds of BH-*trans*-BFCD, BH-*cis*-BFCD and PA6T-Dupont tested by Py-GC/MS (pyrolysis temperatures: 550 and 650 °C).

Retention time (min)	Pyrolysis compounds	BH- <i>trans/cis</i> -BFCD		PA6T-Dupont	
		550 °C	650 °C	550 °C	650 °C
3.1	Benzene	+	+	-	-
4.7	Toluene	+	+	-	+
5.2	Cyclopentanone	-	-	+	+
6.9	Ethylbenzene	+	+	-	+
7.1	p-Xylene	-	-	-	+
10.6	Benzonitrile	-	+	+	+
11.0	Phenol	+	+	-	-
14.2	4-methylbenzonitrile	-	-	+	+
17.0	ethylbenzonitrile	-	-	-	+
17.2	Hexanedinitrile	-	-	+	+
17.6	4-ethenylbenzonitrile	-	-	-	+
19.1	1,4-benzendicarbonitrile	-	-	+	+
22.0	Diphenyl ether	-	+	-	-
22.7	Diphenylmethane	-	+	-	-
24.3	1-metyl-4-phenoxy-benzene	-	+	-	-

28.5 4-phenoxybenzotrile - + - -

+: Compounds was detected; -: Compounds was not detected.

Mechanical Properties

As described in **Table 6**, the tensile strength and Young's modulus of BH-*trans*-BFCD and BH-*cis*-BFCD was 83.6-101.2 MPa and 2.4-2.8 GPa, respectively. BH-*trans*-BFCD showed better mechanical performance than BH-*cis*-BFCD. It is mainly ascribed to its high content hydrogen bond and molecular chain close packing. We also investigated the tensile strength and color change of BH-*trans*-BFCD and BH-*cis*-BFCD which treated at 220 °C for about 1, 3, 5 and 7 h, respectively. Both of the two samples were found to have decreased tensile strength after treating at 220 °C for a certain period (as shown in **Figure 11**). BH-*trans*-BFCD displayed about 20 MPa (20%) reduces while about 30 MPa (36%) decreased for BH-*cis*-BFCD. The reduction magnitude of tensile strength of BH-*cis*-BFCD was much larger than that of BH-*trans*-BFCD. In addition, the tensile strength of BH-*trans*-BFCD treated at 220 °C for 7 h was found to be still much higher than even un-treated BH-*cis*-BFCD. It indicates that BH-*trans*-BFCD has much better tensile strength retention at high temperature than BH-*cis*-BFCD.

In order to investigate this phenomenon, the PLM was carried out to study the samples' aggregation structure (as shown in **Figure 12**). From the PLM images of BH-*trans*-BFCD (annealing at 280 °C for 1 h, 3 h and 5 h under vacuum condition) and BH-*cis*-BFCD (annealing at 280 °C for 5 h under vacuum condition), we observed the micro-fibrous structure. And this micro-fibrous structure got increasingly obvious. But this phenomenon can not be found in the sample of BH-*cis*-BFCD. So BH-*trans*-BFCD had better tensile strength than that of BH-*cis*-BFCD. As shown in **Figure 13**, the color of BH-*cis*-BFCD and BH-*trans*-BFCD became deep but when compared with BH-*cis*-BFCD the color change of BH-*trans*-BFCD was slighter. The deeper color is caused by the content changes of chromophore contained in the compounds. With high temperature treating, BH-*cis*-BFCD got unstable, and generated more chromophore units than BH-*trans*-BFCD. Above all, the tensile strength and color change experiments suggest that the mechanical property and high temperature stability of BH-*trans*-BFCD is much better than BH-*cis*-BFCD. It was in agreement with the results of thermal degradation analysis.

The dynamic mechanical analysis (DMA) was also used to characterize the thermal mechanical properties of BH-*trans*-BFCD and BH-*cis*-BFCD. As shown in **Figure 14**, the glass transition temperature of BH-*trans*-BFCD and BH-*cis*-BFCD was about 273 and 238 °C, respectively. BH-*trans*-BFCD displayed much higher T_g than BH-*cis*-BFCD, which was consistent with the results of DSC measurement. From the storage modulus curves (**Figure 14**) of the two semi-aromatic polyamides, it was found that the prepared polymers had good thermal mechanical property. Their storage modulus only decreased a little from 50 °C to the glass transition temperature of the polymers. BH-*trans*-BFCD and BH-*cis*-BFCD showed a storage

modulus about 1.3 GPa (at 250 °C) and 1.2 GPa (at 220 °C), respectively. It suggests that the prepared semi-aromatic polyamides possess good thermal mechanical properties.

Table 6 Tensile and thermal properties of BH-*trans*-BFCD and BH-*cis*-BFCD.

Polymers	Tensile strength (MPa)	Elongation at yield (%)	Young's modulus (GPa)	Storage modulus at 220 °C (GPa)	Glass Transition Temperature ^a (°C)
BH- <i>trans</i> -BFCD	101.2	17.5	2.8	1.4	273.7
BH- <i>cis</i> -BFCD	83.6	20.2	2.4	1.2	238.4

^a detected by dynamic mechanical analysis (DMA).

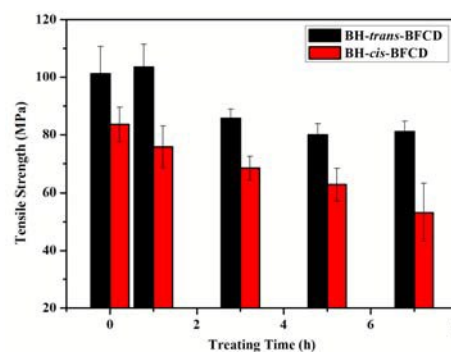


Figure 11 Tensile strength of BH-*trans*-BFCD and BH-*cis*-BFCD treated at 220 °C for 1, 3, 5 and 7 h.

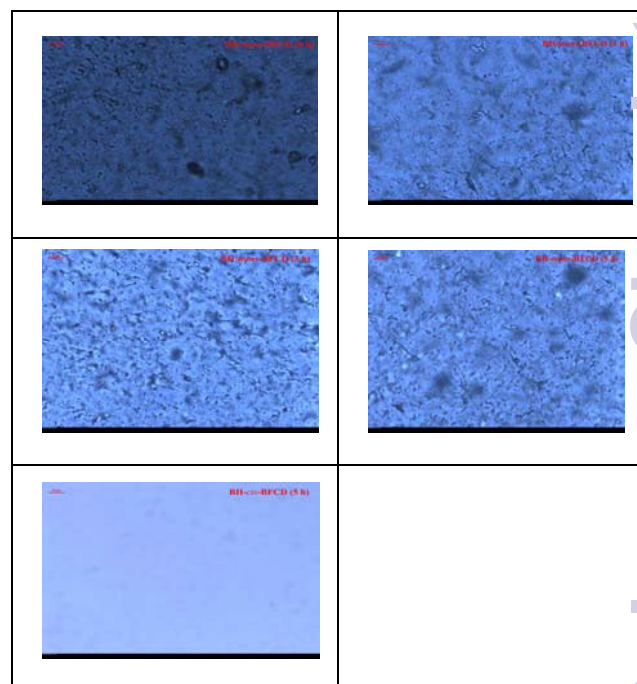


Figure 12 The PLM images of BH-*trans*-BFCD and BH-*cis*-BFCD treated at 280 °C under vacuum for 1, 3 and 5h.

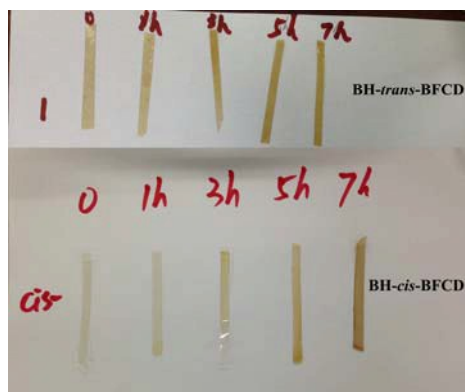


Figure 13 The color change of BH-*trans*-BFCD and BH-*cis*-BFCD treated at 220 °C for 1, 3, 5 and 7 h.

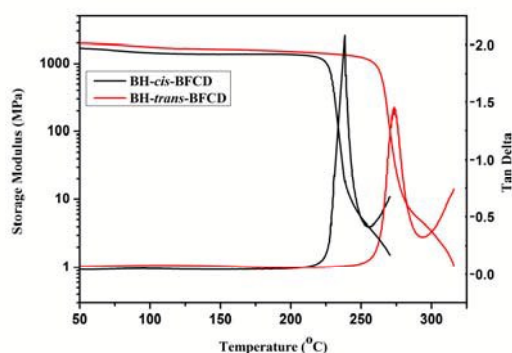


Figure 14 DMA curves (Tan delta and storage modulus) of BH-*trans*-BFCD and BH-*cis*-BFCD.

Rheological Properties of Polymers

The rheological properties of the resultant semi-aromatic polyamides were characterized with a parallel plate rheometer. In order to investigate the suitable melting process window of the two semi-aromatic polyamides, the temperature sweep (as shown in **Figure 15** and **Figure 16**) was conducted to analysis their complex viscosities, storage modulus (G') and loss modulus (G''). **Figure 15** shows that the complex viscosity of BH-*cis*-BFCD is much lower. The main reason is that the *cis*-chemical structure of BH-*cis*-BFCD displays a much larger molecular volume than BH-*trans*-BFCD. So BH-*cis*-BFCD shows a much lower viscosity between this two samples. As shown in **Figure 16**, the melt loss modulus (G'') of BH-*cis*-BFCD was almost larger than the storage modulus (G') during the testing temperature. It also found that the melt loss modulus of BH-*trans*-BFCD was larger than the storage modulus at about 305 °C. It suggests these two samples can be melt process above this temperature (intersection point of G' and G'').

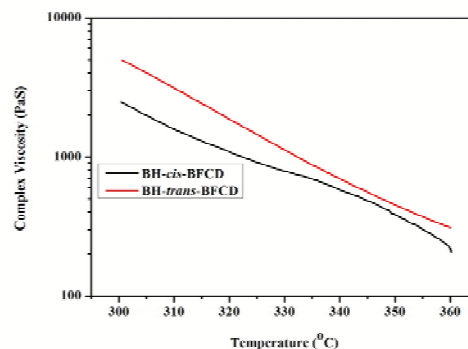


Figure 15 Plot of complex viscosities versus temperature for BH-*trans*-BFCD and BH-*cis*-BFCD.

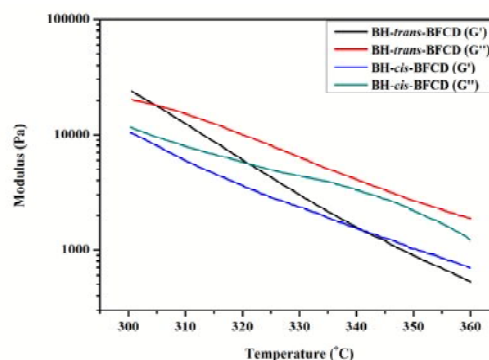


Figure 16 Storage modulus and loss modulus curves versus temperature for BH-*trans*-BFCD and BH-*cis*-BFCD.

As shown in **Figure 17** and **Figure 18**, the time sweep was used to calculate the melt stability of these samples. The complex viscosity of BH-*trans*-BFCD was kept almost unchanging from beginning to the end of the test experiment while it increased gradually for the BH-*cis*-BFCD. The main reason of the above phenomenon is that the oxygen is easy to permeate into the molecular chain of BH-*cis*-BFCD which has loose chemical structure. Then the probability of oxidation reaction gets much higher. Also the the melt storage modulus (G') and loss modulus value (G'') of BH-*cis*-BFCD and BH-*trans*-BFCD were investigated (as show in **Figure 18**). The value of G'' of BH-*cis*-BFCD and BH-*trans*-BFCD was always larger than G' . The intersection point of melt storage modulus (G') and loss modulus value (G'') did not appear during the whole testing period. It suggests that BH-*cis*-BFCD and BH-*trans*-BFCD display similar good melt stability.

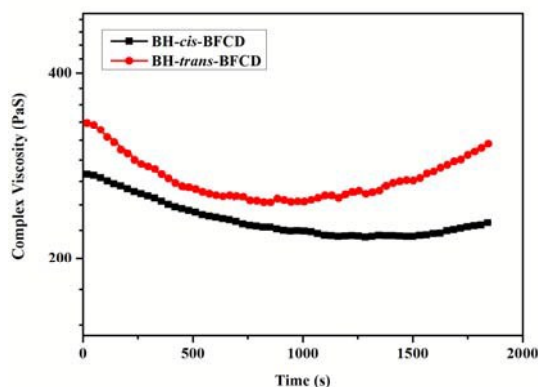


Figure 17 Plot of complex viscosities versus time (at 330 °C) for BH-*trans*-BFCD and BH-*cis*-BFCD.

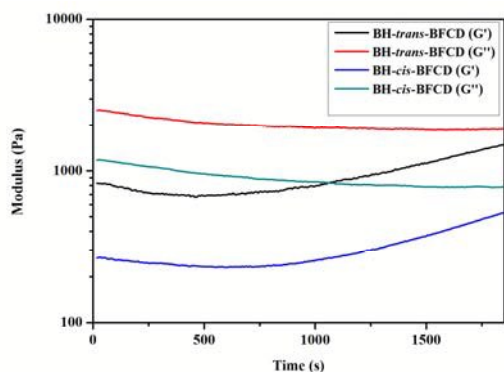


Figure 18 Storage modulus and loss modulus curves versus time for BH-*trans*-BFCD and BH-*cis*-BFCD.

Conclusions

Semi-aromatic amide monomers containing stable *trans*- or *cis*-cyclohexane unit was synthesized with a facile interface reaction at ambient temperature. It was then used to react with BHPPE with bulky group by nucleophilic polycondensation to synthesize a kind of semi-aromatic polyamides, named BH-*trans*-BFCD and BH-*cis*-BFCD. It was found that the glass transition temperature, thermal stability and melting stability of BH-*trans*-BFCD was much higher than that of BH-*cis*-BFCD because of its close packing and large content hydrogen bond of polymer chain of BH-*trans*-BFCD. Also the sample of BH-*trans*-BFCD was found to have better mechanical property than that of BH-*cis*-BFCD for its micro-fibrous structure. Additionally, the resultant semi-aromatic polyamides displayed high thermal stability when compared with the commercial materials PA6T-Dupont. Therefore, these semi-aromatic polyamides could be potentially used as heat resistant thermoplastic materials especially when the thin-walled work-piece and excellent durability are required.

Experimental

Materials

N-methyl-2-pyrrolidone (NMP) (ShanDong YuNeng Chemical Industry Company), 4-FBC (99.5%, Lanning Chemical Company Limited), sodium hydroxide (NaOH) (AR, KeLong Chemical Reagent Company), 1,4-*trans*-cyclohexanediamine (99%, BeiSiTe Chemical Reagent Company), 1,4-*cis*-cyclohexanediamine (99%, FuErSiTe Chemical Reagent Company), PA6T-Dupont (DuPont Company, 18502 NC010) and other reagents were obtained commercially, BHPPE was synthesized as reported earlier by our group [39].

Monomer synthesis

N,N'-Bis(4-fluorobenzoyl) *trans*-cyclohexanediamine (*trans*-BFCD) (as shown in Scheme 1)

Firstly, 1 L mixture of dichloromethane and 4-FBC (317 g, 2 mol) was added into a 5 L three-necked round bottom flask. Next, the solution of 1,4-*trans*-cyclohexanediamine (114 g, 1 mol), NaOH (80 g, 2 mol) and sodium dodecyl sulfate (3 g) dissolved in deionized water (1000 ml) was added dropwisely during 2 h. Then the reaction was kept at ambient temperature under stirring for about 8 h to yield a white mixture. Afterwards, the mixture was evaporated at 50 °C to recover the solvent CH₂Cl₂. Then the slurry mixture was filtered to collect the solid crude product. The crude product was washed with hot deionized water for three times to remove the byproduct and un-reacted reagent. Then it was recrystallized from N,N-dimethylformamide (DMF) to form a needlelike crystal. Finally it was dried at 80 °C in an oven under vacuum. Yield: 311.1 g (86.9%). FT-IR (KBr, cm⁻¹): 3328 cm⁻¹ (N-H), 1631 cm⁻¹ (-CO-), 3074 cm⁻¹ (C-H aromatic ring), 2929, 2852 cm⁻¹ (-CH₂-), 1601, 1499 cm⁻¹ (C=C of aromatic ring), 1228 cm⁻¹ (C-N), 855 cm⁻¹ (para substitution of the benzene ring). ¹H-NMR [400 MHz, deuterated DMSO-d₆/ TMS, ppm]: 1.428-1.477 (t, 4H, H1), 1.891-1.907 (d, 4H, H2), 3.764 (s, 2H, H3), 7.269-7.313 (t, 4H, H4), 7.901-7.936 (m, 4H, H5), 8.287-8.307 (d, 2H, H6).

N,N'-Bis(4-fluorobenzoyl) *cis*-cyclohexanediamine (*cis*-BFCD)

1,4-*cis*-BFCD was obtained as following the general synthesis procedure as *trans*-BFCD after reaction of 4-FBC with 1,4-*cis*-cyclohexanediamine. The crude product was recrystallized from ethanol to form square granulated crystal. Yield: 303.2 g (84.7%). FT-IR (KBr, cm⁻¹): 3304 cm⁻¹ (N-H), 1637 cm⁻¹ (-CO-), 3073 cm⁻¹ (C-H of aromatic ring), 2932, 2855 cm⁻¹ (-CH₂-), 1603, 1500 cm⁻¹ (C=C of aromatic ring), 1233 cm⁻¹ (C-N), 848 cm⁻¹ (para substitution of the benzene ring). ¹H-NMR [400 MHz, deuterated DMSO-d₆/ TMS, ppm]: 1.629-1.657 (m, 4H, H1), 1.833-1.878 (m, 4H, H2), 3.878 (s, 2H, H3), 7.266-7.310 (m, 4H, H4), 7.914-7.950 (m, 4H, H5), 8.084-8.100 (d, 2H, H6).

Polymer synthesis

Synthesis of BH-*trans*-BFCD

The polymerizations (as shown in Scheme 2) were performed in a 500 mL three-necked round-bottom flask fitted with a mechanical stirrer. Equimolar amounts of *trans*-BFCD (35.8 g, 0.1 mol) and BHPPE (29 g, 0.1 mol) and NMP (200 ml) were added into the reactor together with toluene (10 ml) as water carrier and potassium carbonate (16.6 g, 0.12 mol) as base.

The mixture was heated to 160-180 °C to remove the reaction byproduct water for about 1-2 h. That is beneficial for the conversion of oligomers. Next, the reaction temperature was kept at 202 °C for 10 h to allow for the formation of high molecular weight polymers. Then the viscous reaction solution was poured into water to precipitate fibrous polymer. It was crushed into powder and washed with hot deionized water repeatedly to remove the KF formed during the polymerization procedure. Finally it was dried at 100 °C in an oven under vacuum for 12 h.

BH-*cis*-BFGD was obtained following the similar synthesis procedure as BH-*trans*-BFGD.

Characterization

Intrinsic viscosity analysis: the intrinsic viscosity (η_{int}) of polymers was measured by a Cannon-Ubbelodde viscometer at 30±0.1 °C. Polymer solution was prepared by dissolving 0.500 g polymer into 100 ml NMP. The results were obtained by the one-point method (or Solomon-Ciuta equation) as follows:

$$\eta_{int} = \frac{\sqrt{2(\eta_{sp} - \ln \eta_r)}}{C}$$

where $\eta_r = \eta/\eta_0$, $\eta_{sp} = \eta/\eta_0 - 1$.

Chemical structure analysis:

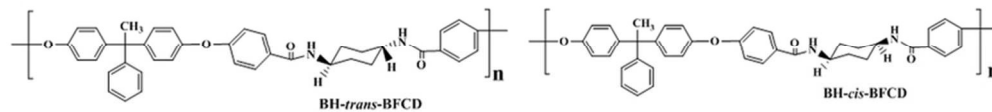
FT-IR spectroscopic measurement was performed on a NEXUS670 FT-IR instrument. ¹H-NMR spectra were obtained on a Bruker-400 NMR spectrometer. Thermal analysis: Differential scanning calorimetry (DSC) measurements were determined by a NETZSCH DSC 200 PC thermal analysis instrument. The heating rate was 10 °C/min under nitrogen atmosphere. Thermogravimetric analysis (TGA) measurements were determined by a TGA Q500 V6.4 Build 193 thermal analysis instrument at different heating rate of 5, 10, 20 and 40 °C/min under nitrogen atmosphere, respectively. Mechanical testing: the stress-strain behaviour of the resultant polymers was measured with an Instron Corporation 4302 instrument at room temperature. The specification of the sheet specimens was 50 mm × 3 mm × 3 mm (length × width × thickness) and five replicas were prepared for every sample. An average value of five replicas was used. Polarized light microscopy (PLM BX51) was used to determine the aggregation structure of the samples. A dynamic mechanical analysis (DMA, TA-Q800) was used to investigate the samples' thermal mechanical properties with a tensile mode at a frequency of 1 Hz with a heating rate of 5 °C/min. Rheological testing (disk sample with diameter of 3 cm and thickness of 1mm): a Parallel plate rheometer (Bohlin Gemini 200, Britain) fitted with 2.5 cm diameter stainless steel parallel plates was performed to characterize the samples' melt flowability with the scanning model based on temperature (temperature scanning rate: 5 °C/min, shear strain: 2%, shear frequency: 1 Hz) and time (shear strain: 2%, shear frequency: 1 Hz). Thermal degradation mechanism: the Py/GC-MS spectrometry was carried out to study the degradation mechanism of the

resultant semi-aromatic polyamides with different pyrolysis temperature (550 °C and 650 °C).

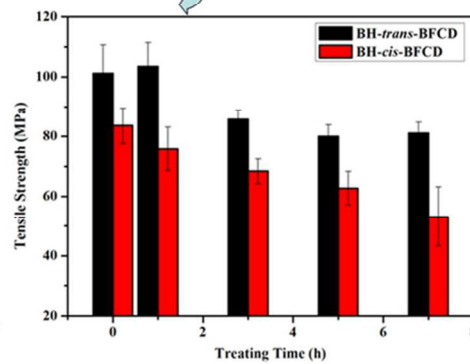
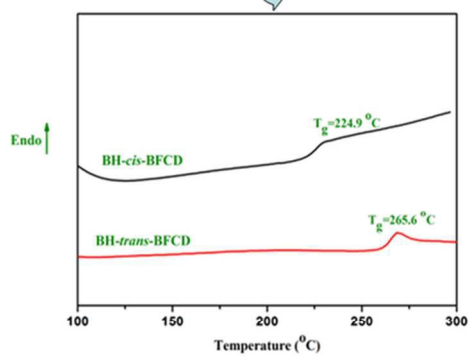
Notes and References

- (1) José, M. G.; Félix, C.; García, F. S.; José, L. de la P. High-performance aromatic polyamides. *Prog. in Polym. Sci.* **2010**, *35*, 623-638.
- (2) Crespo, L.; Sanclimens, G.; Pons, M.; Giral, E.; Royo, M.; Albericio, F. Peptide and Amide Bond-Containing Dendrimers. *Chem. Rev.*, **2005**, *105*, 1663-1681.
- (3) Zhang, G.; Bai, D. T.; Li, D. S.; Long, S. R.; Wang, X. J.; Yang, Jie. Synthesis and properties of polyamides derived from 4,6-bis(4-chloroformylphenylthio) pyrimidine and 3,6-bis(4-chloroformylphenylthio) pyridazine. *Polym. Intern.* **2013**, *62*: 1358-1367.
- (4) Du, S. M.; Wang, W. B.; Yan, Y.; Zhang, J.; Tian, M.; Zhang L. Q.; Wan, X. H. A facile synthetic route to poly(p-phenylene terephthalamide) with dual functional groups. *Chem. Commun.*, **2014**, *50*, 9929-9931.
- (5) Williams, J. C.; Meador, M. Ann B.; McCorkle, L.; Mueller, Carl.; Wilmoth, N. Synthesis and Properties of Step-Growth Polyamide Aerogels Crosslinked with Triacid Chlorides. *Chem. Mater.* **2014**, *26*, 4163-4171.
- (6) Hsiao, S. H.; Chen, C. W.; Liou, G. S. Novel aromatic polyamides bearing pendent diphenylamino or carbazolyl groups. *J. Polym. Sci., Part A: Polym. Chem.*, **2004**, *42*, 3302-3313.
- (7) Liou, G. S.; Lin, H. Y.; Yen, H. J. Synthesis and characterization of electroactive hyperbranched aromatic polyamides based on A2B-type triphenylamine moieties. *J. Mater. Chem.* **2009**, *19*, 7666-7673.
- (8) Rao, Y.; Waddon, A. J.; Farris, R. J. Structure-property relation in poly(p-phenylene terephthalamide) (PPTA) fibers. *Polymer* **2001**, *42*, 5937-5946.
- (9) Ferreira, J. J.; dela, C. J. G.; Lozano, A. E.; de, A. J. Polyisophthalamides with heteroaromatic pendent rings: synthesis, physical properties, and water uptake. *J. Polym. Sci. Part A: Polym. Chem.* **2005**, *43*, 5300-5311.
- (10) Uddin, A. J.; Ohkoshi, Y.; Gotoh, Y.; Nagura, M.; Hara, T. Influence of moisture on the viscoelastic relaxations in long aliphatic chain contained semiaromatic polyamide, (PA9-T) fiber. *J. Polym. Sci. Part B: Polym. Phys.* **2003**, *41*, 2878-2891.
- (11) Uddin, A. J.; Ohkoshi, Y.; Gotoh, Y.; Nagura, M.; Hara, T. Melt spinning and laser-heated drawing of a new semiaromatic polyamide, PA9-T fiber. *J. Polym. Sci. Part B: Polym. Phys.* **2004**, *42*, 433-444.
- (12) Uddin, A. J.; Gotoh, Y.; Ohkoshi, Y.; Nagura, M.; Endo, R.; Hara, T. Hydration in a new semiaromatic polyamide observed by humidity-controlled dynamic viscoelastometry and X-ray diffraction. *J. Polym. Sci. Part B: Polym. Phys.* **2005**, *43*, 1640-1648.
- (13) Uddin, A. J.; Ohkoshi, Y.; Gotoh, Y.; Nagura, M.; Endo, R.; Hara, T. Effects of take-up speed of melt spinning on the structure and mechanical properties of maximally laser drawn PA9-T fibers. *Inter. Polym. Proce.* **2006**, *21*, 263-271.

- (14) Uddin, A. J.; Gotoh, Y.; Ohkoshi, Y.; Nishino, T.; Endo, R.; Crystal Modulus of a New Semiaromatic Polyamide 9-T. *Polym. Eng. Sci.* **2012**, *52*, 331-337.
- (15) Zhang, C. H.; Huang, X. B.; Zeng, X. B.; Cao, M.; Cai, T. M.; Jiang, S. J.; Yi, Q. F. Fluidity Improvement of Semiaromatic Polyamides: Modification with Oligomers. *J. Appl. Polym. Sci.* **2014**, *7*, DOI: 10.1002/APP.40058.
- (16) Wang, W. Z.; Zhang, Y. H. Synthesis of semiaromatic polyamides based on decanediamine. *Chinese J. Polym. Sci.* **2010**, *4*, 467-473.
- (17) Ballistreri, A.; Garozzo, D.; Giuffrida, M.; Maravigna, P. Thermal decomposition processes in aliphatic-aromatic polyamides investigated by mass spectrometry. *Macromolecules* **1986**, *19*, 2693-2699.
- (18) Shabanian, M.; Kang, N. J.; Liu, J. W.; Wagenknecht, U.; Heinrich, G.; Wang, D. Y. Bio-based semi-aromatic polyamide/functional clay nanocomposites: preparation and properties. *RSC Adv.*, **2014**, *4*, 23420-23427.
- (19) Zhang, G.; Huang, G. S.; Li, D. S.; Wang, X. J.; Long, S. R.; Yang, J. Facile Synthesis of Processable Semiaromatic Polyamides Containing Thioether Units. *Ind. Eng. Chem. Res.* **2011**, *50*, 7056-7064.
- (20) Wilsens, Carolus H. R. M.; Deshmukh, Yogesh S.; Noorder, Bart A. J.; Rastogi, S. Influence of the 2,5-Furandicarboxamide Moiety on Hydrogen Bonding in Aliphatic-Aromatic Poly(ester amide)s. *Macromolecules* **2014**, *47*, 6196-6206.
- (21) Harashina, H.; Nakane, T.; Itoh, T. Synthesis of Poly(ester amide)s by the Melt Polycondensation of Semiaromatic Polyesters with Ethanolamine and Their Characterization. *J. Polym. Sci., Part A: Polym. Chem.* **2007**, *11*, 2184-2193.
- (22) Yang, S. H.; Fu, P.; Liu, M. Y.; Wang, Y. D.; Zhang, Y. C.; Zhao, Q. X. Synthesis, characterization of polytridecamethylene 2,6-naphthalamide as semiaromatic polyamide containing naphthalene-ring. *Expre. Polym. Lett.* **2010**, *4*, 442-449.
- (23) Wang, W. Z.; Wang, X. W.; Li, R. X.; Liu, B. Y.; Wang, E. G.; Zhang, Y. H. Environment-Friendly Synthesis of Long Chain Semiaromatic Polyamides with High Heat Resistance. *J. Appl. Polym. Sci.* **2009**, *114*, 2036-2042.
- (24) Novitsky, T. F.; Lange, C.A.; Mathias, L.J.; Osborn, S.; Ayotte, R.; Manning, S. Eutectic melting behavior of polyamide 10,T-co-6,T and 12,T-co-6,T copolyterephthalamides. *Polymer* **2010**, *51*, 2417-2425.
- (25) Liu, M. Y.; Li, K. F.; Yang, S. H.; Fu, P.; Wang, Y. D.; Zhao, Q. X. Synthesis and Thermal Decomposition of Poly(dodecamethylene terephthalamide). *J. Appl. Polym. Sci.*, **2011**, *122*, 3369-3376.
- (26) Wang, W. Z.; Zhang, Y. H. Environment-friendly synthesis of long chain semiaromatic polyamides. *Express Polym. Lett.* **2009**, *8*, 470-476.
- (27) Liaw, D. J.; Chang, F. C.; Leung, M. K.; Chou, M. Y.; Muellen, K. High thermal stability and rigid rod of novel organosoluble polyimides and polyamides based on bulky and noncoplanar naphthalene-biphenyldiamine. *Macromolecules* **2005**, *38*, 4024-4029.
- (28) Moisa, S.; Landsberg, G.; Rittel, D.; Halary, J.L. Hysteretic thermal behavior of amorphous semi-aromatic polyamides. *Polymer* **2005**, *46*, 11870-11875.
- (29) Shabbir, S.; Zulfqar, S.; M.; Sarwar, M. I. Amine-terminated aromatic and semi-aromatic hyperbranched polyamides: synthesis and characterization. *J. Polym. Res.* **2011**, *18*, 1919-1929.
- (30) Shabbir, S.; Zulfqar, S.; Zahoor, A.; M.; Sarwar, M. I. Pyrimidine based carboxylic acid terminated aromatic and semiaromatic hyperbranched polyamide-esters: synthesis and characterization. *Tetrahedron* **2010**, *66*, 7204-7212.
- (31) Liaw, D. J.; Hsu, P. N.; Chen, W. H.; Lin, S. L. Synthesis and Properties of New Soluble Polyamides Derived from 2,2'-Dimethyl-4,4'-bis(4-carboxyphenoxy) biphenyl. *Macromolecules*. **2002**, *35*, 4669-4676.
- (32) Zhang, G.; Zhou, Y. X.; Kong, Y.; Li, Z. M.; Long, S. R.; Yang, J. Semiaromatic polyamides containing ether and different numbers of methylene (2-10) units: synthesis and properties. *RSC Advances*, **2014**, *4*, 63006-63015.
- (33) Zhang, G.; Zhou, Y. X.; Li, Y.; Wang, X. J.; Long, S. R.; Yang, J. Investigation of the synthesis and properties of isophorone and ether units based semi-aromatic Polyamides. *RSC Advances*, **2015**, *5*, 49958-49967.
- (34) Ivanysenko, O.; Strandman, S.; Zhu, X. X. Triazole-linked polyamides and polyesters derived from cholic acid. *Polym. Chem.*, **2012**, *3*, 1962-1965.
- (35) Shabanian, M.; Kang, N. J.; Wang, D. Y.; Wagenknecht, U.; Heinrich, G. Synthesis, characterization and properties of novel aliphatic-aromatic polyamide/functional carbon nanotube nanocomposites via in situ polymerization. *RSC Adv.* **2013**, *3*, 20738-20745.
- (36) Huang, H. Y.; Lee, Y. T.; Yeh, L. C.; Jian, J. W.; Huang, T. C.; Liang, H. T.; Yeh, J. M.; Chou, Y. C. Photoactively electroactive polyamide with azo group in the main chain via oxidative coupling polymerization. *Polym. Chem.* **2013**, *4*, 343-350.
- (37) Matsunaga, D.; Tamaki, T.; Ichimura, K. Azo-pendant polyamides which have the potential to photoalign chromonic lyotropic liquid crystals. *J. Mater. Chem.* **2003**, *13*, 1558-1564.
- (38) Kissinger, H. E. Reaction Kinetics in Differential Thermal Analysis. *Anal. Chem.* **1957**, *29*, 1702-1706.
- (39) Zhang, G.; Xing, X. J.; Li, D. S.; Wang, X. J.; Yang, J. Effects of thioether content on the solubility and thermal properties of aromatic polyesters. *Industrial & Engineering Chem. Res.* **2013**, *52*, 16577-16584.



The different confirmation brought surprising materials' property.



37x28mm (600 x 600 DPI)